Journal of Superconductivity and Novel Magnetism
https://doi.org/10.1007/s10948-019-05333-z

ORIGINAL PAPER

Highly Isotropic In-plane Upper Critical Field in the Anisotropic *s*-Wave Superconductor 2*H*-$NbSe_2$

Syuma Yasuzuka[1] · Shinya Uji[2] · Shiori Sugiura[2,5] · Taichi Terashima[2] · Yoshio Nogami[3] · Koichi Ichimura[4] · Satoshi Tanda[4]

Received: 12 June 2019 / Accepted: 1 October 2019

Abstract
Resistivity measurements for a layered transition metal dichalcogenide 2H-$NbSe_2$ were performed to investigate the in-plane anisotropy of the upper critical field (H_{c2}) for magnetic fields up to 14.5 T at temperatures down to 2.0 K. For fields rotated within the basal plane, the in-plane anisotropy of a characteristic field H^* (defined as the field strength at which the resistivity reaches zero) showed twofold symmetry at low temperatures. On the basis of this result, the in-plane anisotropy of H_{c2} and the superconducting gap structure in 2H-$NbSe_2$ are discussed.

Keywords 2H-$NbSe_2$ · Upper critical field · Anisotropic s-wave superconductivity · Superconducting gap

1 Introduction

In quasi-two-dimensional (Q2D) transition metal dichalcogenides (TMDs), the physical properties originating from strong electron-phonon interactions and low dimensionality are of great interest. Among the many layered TMDs, 2H-$NbSe_2$ (hereafter referred to as "$NbSe_2$") is one of the most intriguing systems [1–7] because a 2D charge-density-wave (CDW) phase transition occurs at $T_{\mathrm{CDW}} = 33.5$ K [8], followed by a phonon mediated superconducting (SC) transition at $T_c = 7.2$ K [9]. According to band-structure calculations [10], there are several FS sheets: a small Γ-centered Fermi pocket derived from the Se 4p band and larger nearly 2D FS sheets from the Nb 4d bands centered on the $\Gamma(A)$ and $K(H)$ points. Experimental results of the de Haas−van Alphen (dHvA) effect [10] and angle-resolved photoemission spectroscopy (ARPES) [3] are consistent with these band-structure calculations. Studies of superconductivity in $NbSe_2$ have been performed via various experimental methods, such as the tunneling spectroscopy [11], specific heat [12, 13], heat transport [14], London penetration depth measurements [15], scanning tunneling microscopy (STM) [16, 17], and ARPES [18, 19] to investigate deviations from the conventional Bardeen-Cooper-Schrieffer (BCS) behavior. A sixfold tail structure has been observed around the vortex cores in STM spectra [11], indicating the presence of an anisotropic s-wave gap structure with sixfold symmetry, which is consistent with ARPES measurements [18].

The dependence of the upper critical field (H_{c2}) on the magnetic field orientation is known to provide valuable information into the SC gap anisotropy. In this case, the observed anisotropy of H_{c2} is often compared with that deduced from the linearized Ginzburg-Landau equation assuming the symmetry of the gap function [20]. For a d-wave SC order parameter, H_{c2} maxima appear when the magnetic field in the real space is parallel to the antinodal directions [20–23]. Similar behavior is found for an anisotropic s-wave superconductivity: the upper critical fields for anisotropic s-wave superconductors $LuNi_2B_2C$ and YNi_2B_2C exhibit clear fourfold symmetry within the basal plane, which is reminiscent of d-wave superconductors [24, 25]. In spite of extensive studies on the superconductivity of $NbSe_2$, it remains unclear whether or not the in-plane anisotropy of H_{c2} shows the sixfold symmetry within the basal plane. Thus, it is of great interest to investigate the in-plane anisotropy of H_{c2} for $NbSe_2$.

✉ Syuma Yasuzuka
yasuzuka@cc.it-hiroshima.ac.jp

1 Research Center for Condensed Matter Physics, Hiroshima Institute of Technology, Hiroshima 731-5193, Japan

2 National Institute for Materials Science, Tsukuba, Ibaraki 305-0003, Japan

3 Department of Physics, Okayama University, Okayama 700-8530, Japan

4 Department of Applied Physics, Hokkaido University, Kita 13, Nishi 8, Kita-ku Sapporo 060-8628, Japan

5 Present address: Institute for Materials Research, Tohoku University, Sendai 980-8577, Japan

In this paper, we report in-plane anisotropy of a characteristic field H^* (where the resistivity reaches zero) of $NbSe_2$ at magnetic fields up to 14.5 T and temperatures down to 2.0 K. For fields rotated within the basal plane, we observed the in-plane anisotropy of H^*, with twofold-symmetric periodicity at low temperatures. On the basis of these results, the in-plane anisotropy of H_{c2} and its interplay with the anisotropic gap structure are discussed.

2 Experimental Methods

Single crystals of $NbSe_2$ were synthesized by the iodine vapor transport method in a sealed quartz tube using Nb wire with a purity of 99.9% and Se shots of 99.999%. The single crystals were cut into a rectangular form ($0.90 \times 0.25 \times 0.02$ mm^3) with a razor blade. In our experiments, the crystal orientation was carefully verified by X-ray diffraction. In-plane resistivity was measured by a conventional four-probe AC technique with an electric current along the a-axis. We used a two-axis rotator in a ^{4}He cryostat with a 17-T SC magnet. The field direction is specified by the polar angle θ and the azimuthal angle ϕ, where θ is the angle between the field and the c-axis and ϕ is the inclination from the b'-axis perpendicular to the a-axis within the basal plane [inset of Fig. 2]. Two single crystals denoted as samples A and B were examined to assess the reproducibility. The residual resistivity ratio (RRR), defined as $\rho_{300\,\mathrm{K}}/\rho_{8\,\mathrm{K}}$, was 31 for sample A, and 34 for sample B. The sample properties are summarized in Table 1.

3 Results

Figure 1 shows the temperature dependence of the resistivity for sample B at magnetic fields of up to 14.5 T. At $\mu_0 H = 0$ T, the resistivity near T_c varies from 10 to 90% of the normal-state value over a narrow range of the approximate $\pm$ 0.1 K centered at $T_c = 7.3$ K. With increasing magnetic field, the resistivity curves shift to lower temperatures. Resistivity anomaly is found at around the CDW transition, $T_{\mathrm{CDW}} = 33.5$ K. For simplicity, the dip position in the $d\rho/dT$ is defined as T_{CDW}, as shown by the inset of Fig. 1. Similar sharp SC and CDW transitions were observed for sample A (not shown here). In the magnetic fields, the resistivity is enhanced below T_{CDW} but T_{CDW} is independent

Table 1 Properties of two single crystals of $NbSe_2$

Sample	$\rho_{8\,\mathrm{K}}$ ($\mu\Omega$ cm)	RRR	T_c (K)	T_{CDW} (K)
A	10.6	31	7.3	33.5
B	8.6	34	7.3	33.5

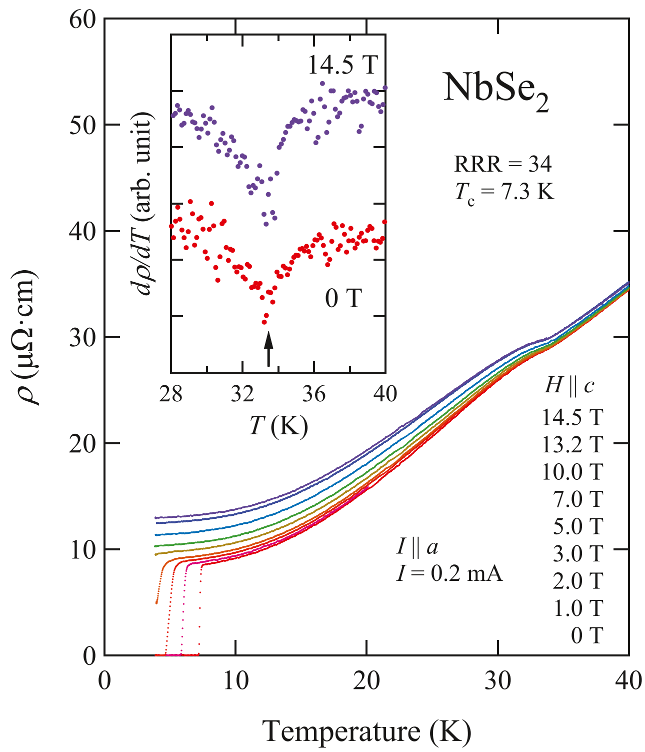

Fig. 1 Temperature dependence of the resistivity for sample B in magnetic fields ranging from 0 to 14.5 T. The inset shows the temperature dependence of the $d\rho/dT$ at 0 T and 14.5 T. The dips indicated by arrows define the CDW transition temperatures, T_{CDW}

of the magnetic fields of up to 14.5 T. All the behavior is consistent with those reported by others [26–28]. We note that positive magnetoresistance is evident up to relatively high temperatures, which also suggests the high quality of our single-crystal samples.

Figure 2a shows the resistivity of sample B as a function of the field angle θ under the magnetic field of 10.5 T, where the field is rotated from positive to negative angles at $\phi = -110°$. We observe deep minima due to the superconductivity for the magnetic field nearly parallel to the basal plane ($\theta = \pm 90°$), while a large magnetoresistance is observed for fields perpendicular to the layers ($\theta = 0°$). This behavior is consistent with the previous report by Morris et al [29]. We do not find dip structures and shallow minimum arising from flux pinning at around $\theta = 0°$, which is another good sign of the high -quality samples [29]. These features in Fig. 2a show that our single-crystal samples are suitable for magnetotransport studies. At around $\theta = \pm 90°$, asymmetric angular dependence of the resistivity is observed. Origin of the asymmetric behavior is discussed later.

Figure 2b shows the resistivity as a function of the field angle θ at various magnetic fields in the c-b' plane ($\phi = 0°$). With increasing magnetic field, the deep minimum due to the SC transition is gradually

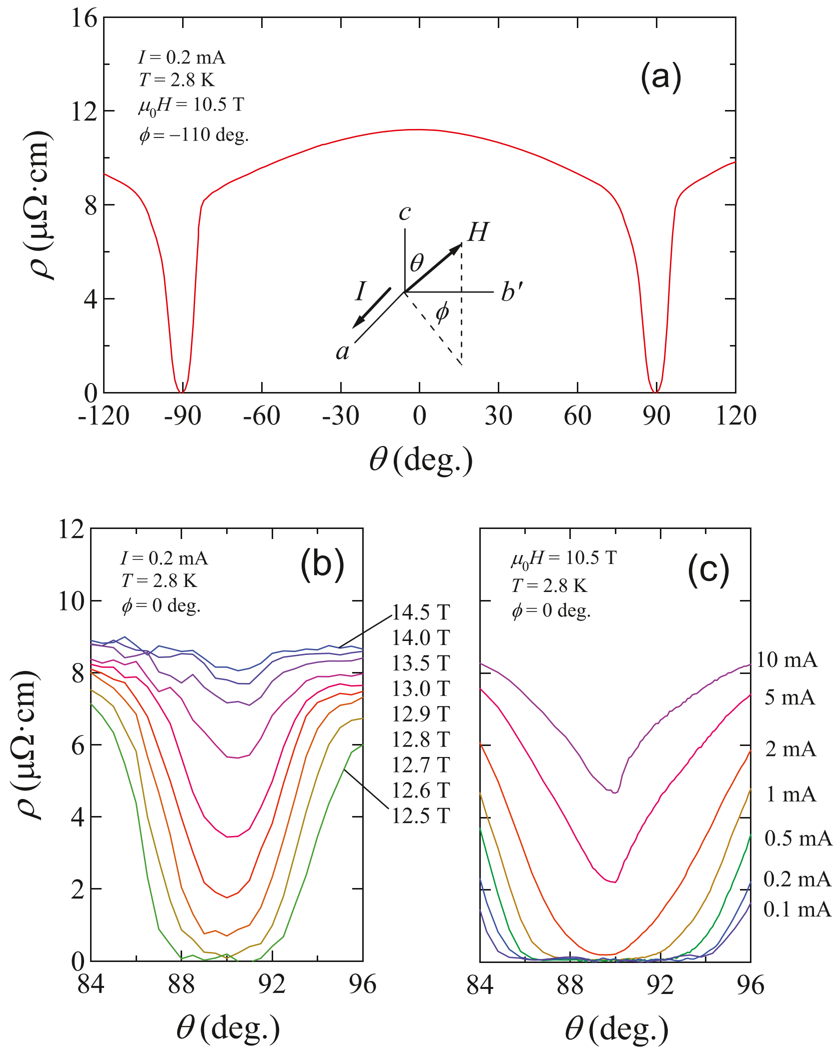

Fig. 2 **a** Resistivity of sample B as a function of the field angle θ under the magnetic field of 10.5 T, where the field is rotated from positive to negative angles at $\phi = -110°$. The angles θ and ϕ are defined in the inset. **b** Resistivity of sample B as a function of the field angle θ in the c-b' plane ($\phi = 0°$) at various fields and **c** at various currents

suppressed. We find that the angular dependence shows slightly asymmetric around $\theta = 90°$. It is known that sample inhomogeneity (geometrical, compositional, structural, etc.) acts as flux pinning centers [30]. Among various origins, some randomness at the sample edges form large energy barriers against the entry and exit of magnetic flux [30]. In the field rotation, the flux pinning at the sample edges likely leads to asymmetric behavior.

Figure 2c shows the resistivity as a function of the field angle θ at various currents. Below 1 mA, the resistivity shows a quasi-sinusoidal angular dependence and the SC state is observed only when the field is nearly parallel to the basal plane ($\theta \approx 90°$). As the current increases further ($I \geq 2$ mA), the asymmetric behavior is enhanced and flux-flow resistance appears even at $\theta = 90°$. Above 5 mA, the $R(\theta)$ curve shows a sharp dip at $\theta = 90°$. When the magnetic field of 10.5 T is applied parallel to the basal plane, the critical current is roughly estimated to be $I_c \sim$ 2 mA (40 A/cm^2), below which the flux-flow resistance is strongly suppressed. For sample A, the critical current is estimated as 1 mA (33 A/cm^2).

Figure 3a shows the in-plane resistivity of sample B as a function of H for various ϕ values within the basal plane at 2.8 K. The current used here is 0.2 mA which is one order of magnitude smaller than the estimated critical current (I_c $\sim$ 2 mA) at $\phi = 0°$ as shown by Fig. 2c. In Fig. 3a, we note that the resistive transition is very sharp, whose width amounts to only $\sim$ 0.4 T. Figure 3b shows the ϕ dependence of the resistivity at 2.8 K derived from the field dependence of the resistivity for a fixed value of ϕ. For the field rotated within the basal plane, a highly isotropic normal-state magnetoresistance is found at 14.5 T. As the magnetic field strength decreases, the field orientation anisotropy of the resistivity increases, whereas the zero resistivity is observed for all ϕ values at 10.6 T. The larger resistivity for $I \perp H$ ($\phi = 0°$) than that for $I \parallel H$ ($\phi = 90°$) show that the Lorentz force plays a dominant role in the origin of the twofold symmetry.

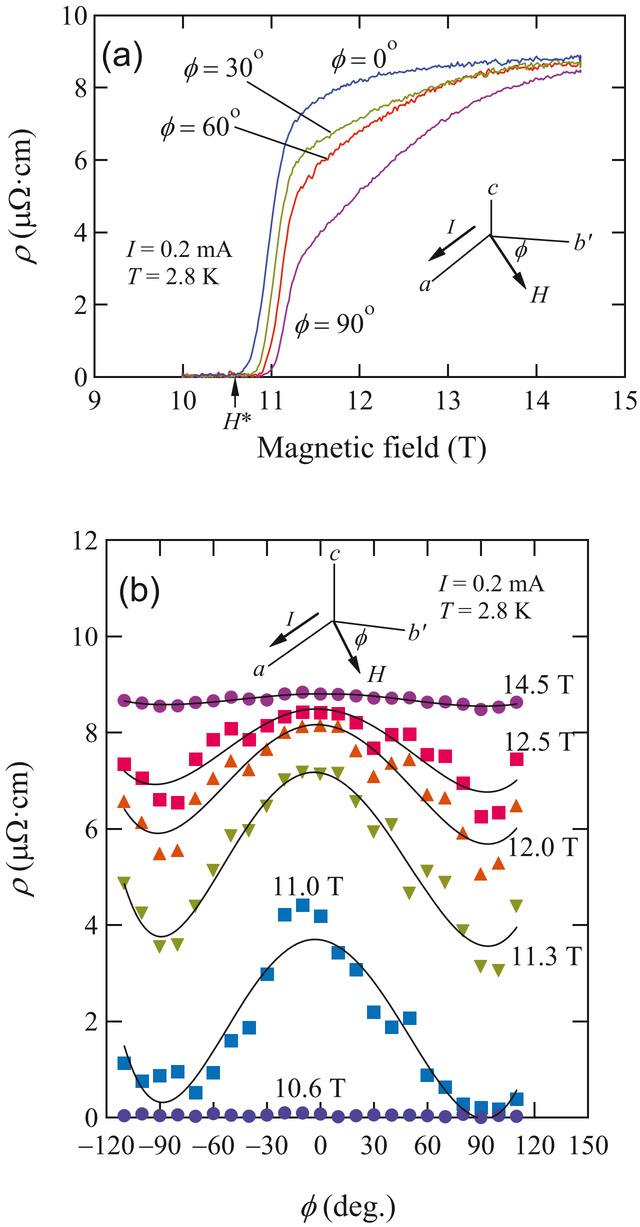

Fig. 3 **a** Resistivity of sample B as a function of the magnetic field H at 2.8 K for various values of ϕ. The characteristic field, H^*, at $\phi = 0°$ is indicated by the arrow. **b** Angular dependence of the resistivity when the magnetic field is rotated within the most highly conducting plane, derived from **a**. The solid curves provide a guide for the eye. The inset shows the definition of magnetic field orientation relative to ϕ

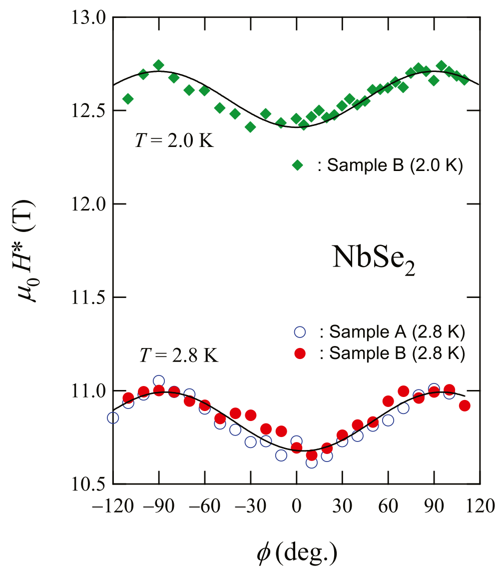

Fig. 4 Characteristic field H^* for both samples derived from the resistive transition vs angle ϕ from b'-axis (see the inset of Fig. 3) at 2.0 and 2.8 K. The solid lines present fits of the date based on a sine function with a periodicity of 180°

To further characterize the in-plane anisotropy in the SC state, we consider the characteristic field H^* which is defined as the field strength at which the resistivity reaches zero. The in-plane anisotropy of H^* is plotted as a function of ϕ in Fig. 4. At 2.8 K, H^* displays twofold symmetry with a maximum value at $\phi = \pm 90°$, corresponding to $I \parallel H$. The same twofold anisotropy is observed at 2.0 K. From the fitting results based on a sine function, the amplitude and average of the H^* anisotropy at $T = 2.8$ K are estimated as $\mu_0 \Delta H^* = 0.17$ T and $\mu_0 \overline{H^*} = 10.8$ T, respectively. Similarly, we obtained $\mu_0 \Delta H^* = 0.15$ T and $\mu_0 \overline{H^*} = 12.6$ T at $T = 2.0$ K.

4 Discussion

Let us discuss the in-plane anisotropy of the intrinsic H_{c2} on the basis of observed $H^*(\phi)$ with twofold symmetry. Because the highly isotropic normal-state magnetoresistance is found at 14.5 T as shown in Fig. 3b, the twofold symmetry in H^* can not be ascribed to the in-plane field dependence of the normal-state resistance [31]. When the magnetic field is not parallel to the current in the vortex liquid regime, the vortices are driven by the Lorentz force, which gives rise to energy dissipation. Because the magnitude of the Lorentz force changes with the angle ϕ in our experimental setup, the angular dependence of the resistance may be affected by the angular dependence of the energy dissipation. It is well known that the Lorentz force picture gives the twofold anisotropy of the resistivity as $\rho(\phi) \propto \sin^2(\phi)$. This $\sin^2(\phi)$ dependence can certainly describe the $\rho(\phi)$ behavior of 90 K YBCO [32] and is explained in terms of SC fluctuation effects in the vortex liquid regime [33]. In this situation, it is unlikely that the anisotropies of both H^* and $\rho(\phi)$ represent that of H_{c2}. After subtracting the twofold symmetry component in Fig. 4, the sixfold symmetry component is less than 2%. Thus, we conclude that the intrinsic H_{c2} may be highly isotropic within the basal plane.

The relationship between the in-plane isotropic nature of the intrinsic H_{c2} and the anisotropic s-wave SC gap structure is next discussed in the following three viewpoints. One is the anisotropy of H_{c2} in the basal plane of a hexagonal crystal [34, 35]. Burlachkov [34] theoretically showed in the basal plane of a hexagonal lattice that there is no anisotropy of H_{c2} near T_c, regardless of the nature of the pairing symmetry. Thus, the obtained isotropic nature in $H_{c2}(\phi)$ may be consistent with the prediction that the sixfold symmetry part of H_{c2} is absent in hexagonal systems. However, we should note that the theory is not directly applicable to $NbSe_2$ because the SC phase coexists with the incommensurate CDW phase. It should be also noted that a clear anisotropy of $H_{c2}(\phi)$ more than 30% in hexagonal material Cs_xWO_3 [36] is inconsistent with the theory.

The second viewpoint is related to the absence of nodes in anisotropic s-wave SC gap structure. According to the ARPES experiment by Kiss et al [18], superconductivity occurs over the Nb-derived FS, with maximal gaps along $\Gamma - K$ and smaller gaps along $\Gamma - M$ (i.e., sixfold symmetry), indicating the anisotropic s-wave superconductivity. Although H_{c2} with the sixfold symmetry is expected [20, 21] from the ARPES measurements [18], only the twofold in-plane anisotropy of H^* is appreciable. The small sixfold symmetry component less than 2% in Fig. 4 shows that the amplitude of the H_{c2} oscillations with sixfold symmetry is significantly reduced in $NbSe_2$ as compared with a d-wave SC gap with nodes [22, 23]. This is because the ARPES experiments [18] suggest the existence of gap minima (i.e., no nodes) in the anisotropic s-wave SC gap for $NbSe_2$.

The third viewpoint is the multiband nature in $NbSe_2$. The multiband effect is neglected in the theories for H_{c2} in d-wave superconductors [20, 21] although the ARPES measurements [19] suggest an anisotropic SC gap with different gap amplitudes in different FS sheets, i.e., two or more types of anisotropic gaps in each FS sheet. Thus, the in-plane anisotropy of H_{c2} in $NbSe_2$ will be averaged out by the different SC gaps.

5 Conclusion

The in-plane angular dependence of H^* showed only twofold symmetry associated with the angular dependence of the Lorentz force. This behavior is likely ascribed to SC fluctuation effects in the vortex liquid regime. On the basis of the in-plane anisotropy of H^*, the amplitude of the H_{c2} oscillation with sixfold anisotropy, if it exists, is much smaller than $\mu_0 \Delta H^* \sim 0.2$ T. These results suggest a highly isotropic H_{c2} within the basal plane. Contrary to expectations, no sixfold symmetry was observed for H_{c2}. The experimental results reported herein demonstrate that the characteristics of the anisotropic s-wave gap in $NbSe_2$, that is, the minimum gap (instead of nodes in a d-wave superconductor) and/or the multiband effect significantly suppress the amplitude of H_{c2} oscillations related to the SC gap anisotropy.

Acknowledgments The authors thank T. Konoike for useful discussion and experimental supports.

References

1. Revolinski, E., Brown, B.E., Beerntsen, D., Armitage, C.H.: The selenide and telluride systems of niobium and tantalum. J. Less-Common Met., 863 (1965)
2. Straub, T.h., Finteis, T.h., Claessen, R., Steiner, P., Hüfner, S., Blaha, P., Oglesby, C.S., Bucher, E.: Charge-density-wave mechanism in 2H−$NbSe_2$: photoemission results. Phys. Rev. Lett. **82**, 4504 (1999)
3. Yokoya, T., Kiss, T., Chainani, A., Shin, S., Nohara, M., Takagi, H.: Fermi surface sheet-dependent superconductivity in 2H-$NbSe_2$. Science **294**, 2518 (2001)
4. Valla, T., Fedorov, A.V., Johnson, P.D., Glans, P.-A., McGuinness, C., Smith, K.E., Andrei, E.Y., Berger, H.: Quasiparticle spectra, charge-density waves, superconductivity, and electron-phonon coupling in 2H-$NbSe_2$. Phys. Rev. Lett. **92**, 086401 (2004)
5. Berthier, C., Molinié, P., Jérome, D.: Evidence for a connection between charge density waves and the pressure enhancement of superconductivity in 2H-$NbSe_2$. Solid State Commun. **18**, 1393 (1976)
6. Neto, A.H.C.: Charge density wave, superconductivity, and anomalous metallic behavior in 2D transition metal dichalcogenides. Phys. Rev. Lett. **86**, 4382 (2001)
7. Inosov, D.S., Zabolotnyy, V.B., Evtushinsky, D.V., Kordyuk, A.A., Büchner, B., Follath, R., Berger, H., Borisenko, S.V.: Fermi surface nesting in several transition metal dichalcogenides. J. Phys. **10**, 125027 (2008)
8. Moncton, D.E., Axe, J.D., DiSalvo, F.J.: Study of superlattice formation in 2H-$NbSe_2$ and 2H-$TaSe_2$ by neutron scattering. Phys. Rev. Lett. **34**, 734 (1975)
9. Harper, J.M.E., Geballe, T.H., DiSalvo, F.J.: Heat capacity of 2H-$NbSe_2$ at the charge density wave transition. Phys. Lett. **54A**, 27 (1975)
10. Corcoran, R., Meeson, P., Onuki, Y., Probst, P.-A., Springford, M., Takita, K., Harima, H., Guo, G.Y., Gyorffy, B.L.: Quantum oscillations in the mixed state of the type II superconductor 2H-$NbSe_2$. J. Phys. Condens. Matter **6**, 4479 (1994)
11. Hess, H.F., Robinson, R.B., Waszczak, J.V.: Vortex-core structure observed with a scanning tunneling microscope. Phys. Rev. Lett. **64**, 2711 (1990)
12. Huang, C.L., Lin, J.-Y., Chang, Y.T., Sun, C.P., Shen, H.Y., Chou, C.C., Berger, H., Lee, T.K., Yang, H.D.: Experimental evidence for a two-gap structure of superconducting $NbSe_2$: a specific-heat study in external magnetic fields. Phys. Rev. B **76**, 212504 (2007)
13. Jing, Y., Lei, S., Yue, W., Zhi-Li, X., Hai-Hu, W.: Quasiparticle density of states of 2H-$NbSe_2$ single crystals revealed by low-temperature specific heat measurements according to a two-component model. Chin. Phys. B **17**, 2229 (2008)
14. Boaknin, E., Tanatar, M.A., Paglione, J., Hawthorn, D., Ronning, F., Hill, R.W., Sutherland, M., Taillefer, L., Sonier, J., Hayden, S.M., Brill, J.W.: Heat conduction in the vortex state of $NbSe_2$: evidence for multiband superconductivity. Phys. Rev. Lett. **90**, 117003 (2003)

15. Fletcher, J.D., Carrington, A., Diener, P., Rodière, P., Brison, P., Prozorov, R., Olheiser, T., Giannetta, R.W.: Penetration depth study of superconducting gap structure of 2H-$NbSe_2$. Phys. Rev. Lett. **98**, 057003 (2007)
16. Rodrigo, J.G., Vieira, S.: STM study of multiband superconductivity in $NbSe_2$ using a superconducting tip. Phys. C **404**, 306 (2004)
17. Noat, Y., Cren, T., Debontridder, F., Roditchev, D., Sacks, W., Toulemonde, P., Miguel, A.: San: Signatures of multigap superconductivity in tunneling spectroscopy. Phys. Rev. B **82**, 014531 (2010)
18. Kiss, T., Yokoya, T., Chainani, A., Hanaguri, T., Nohara, M., Takagi, H.: Charge-order-maximized momentum dependent superconductivity. Nat. Phys. **3**, 720 (2007)
19. Rahn, D.J., Hellmann, S., Kalläne, M., Sohrt, C., Kim, T., Kipp, K.L., Rossnagel, K.: Gaps and kinks in the electronic structure of the superconductor $2H$-$NbSe_2$ from angle-resolved photoemission at 1 K. Phys. Rev. B **85**, 224532 (2012)
20. Takanaka, K., Kuboya, K.: Anisotropy of upper critical field and pairing symmetry. Phys. Rev. Lett. **75**, 323 (1995)
21. Won, H., Maki, K.: Fourfold symmetry of vortex state of d-wave superconductivity and torque magnetometry. Europhys. Lett. **34**, 453 (1996)
22. Yasuzuka, S., Uji, S., Terashima, T., Sugii, K., Isono, T., Iida, Y., Schlueter, J.A.: In-plane anisotropy of upper critical field and flux-flow resistivity in layered organic superconductor β''-$(ET)_2SF_5CH_2CF_2SO_3$. J. Phys. Soc. Jpn. **84**, 094709 (2015)
23. Yasuzuka, S., Koga, H., Yamamura, Y., Saito, K., Uji, S., Terashima, T., Akutsu, H., Yamada, J.: Dimensional crossover and its interplay with in-plane anisotropy of upper critical field in β-$(BDA\text{-}TTP)_2SbF_6$. J. Phys. Soc. Jpn. **86**, 084704 (2017)
24. Metltushko, V., Welp, U., Koshelev, A., Aranson, I., Crabtree, G.W., Canfield, P.C.: Anisotropic upper critical field of $LuNi_2B_2C$. Phys. Rev. Lett. **79**, 1738 (1997)
25. Wang, G.F., Maki, K.: Possible d-wave superconductivity in borocarbides: upper critical field of YNi_2B_2C and $LuNi_2B_2C$. Phys. Rev. B **58**, 6493 (1998)
26. Toyota, N., Nakatsuji, H., Noto, K., Hoshi, A., Kobayashi, N., Muto, Y., Onodera, Y.: Temperature and angular dependences of upper critical fields for the layer structure superconductor 2H-$NbSe_2$. J. Low Temp. Phys. **25**, 485 (1976)
27. Naito, M., Tanaka, S.: Electrical transport properties in $2H$-NbS_2, -$NbSe_2$, -TaS_2, and -$TaSe_2$. J. Phys. Soc. Jpn. **51**, 219 (1982)
28. Nader, A., Monceau, P.: Critical field of 2H-$NbSe_2$ down to 50 mK. SpringerPlus **3**, 16 (2014)
29. Morris, R.C., Coleman, R.V., Bhandari, R.: Superconductivity and magnetoresistance in $NbSe_2$. Phys. Rev. B **5**, 895 (1972)
30. Huebener, R.P.: Motion of magnetic flux structures. In: Gray, K.E. (ed.) Nonequilibrium Superconductivity, Phonon, and Kapitza Boundaries. NATO ASI Series. Plenum, New York (1981)
31. Shimojo, Y., Ishiguro, T., Tanatar, M.A., Kovalev, A.E., Yamochi, H., Saito, G.: Superconducting state of the layered conductor α-$(BEDT\text{-}TTF)_2NH_4Hg(SCN)_4$ in magnetic fields parallel to the layer plane. J. Phys. Soc. Jpn. **71**, 2240 (2002)
32. Kwok, W.K., Welp, U., Crabtree, G.W., Vandervoot, K.G., Hulscher, R., Liu, J.Z.: Direct observation of dissipative flux motion and pinning by twin boundaries in $YBa_2Cu_3O_{7-\delta}$ single crystals. Phys. Rev. Lett. **64**, 966 (1990)
33. Ikeda, R.: Describing fluctuations in the vortex liquid regime. J. Phys. Soc. Jpn. **64**, 1683 (1995)
34. Burlachkov, L.I.: Upper critical field H_{c2} in heavy-fermion superconductors. Sov. Phys. JETP **62**, 800 (1986)
35. Mineev, V.P., Samokhin, K.: Introduction to Unconventional Superconductivity. Gordon and Breach Science Publishers, Amsterdam (1999)
36. Skokan, M.R., Moulton, W.G., Morris, R.C.: Normal and superconducting properties of Cs_xWO_3. Phys. Rev. B **20**, 3670 (1979)